A Planar Printed Nona-Band Loop-Monopole Reconfigurable Antenna for Mobile Handsets

Yu Liu, Peiqin Liu, *Student Member, IEEE*, Zhijun Meng, Lifeng Wang, and Yue Li, *Senior Member, IEEE*

***Abstract*—In this letter, a planar loop-monopole reconfigurable antenna is proposed for mobile handsets with a relative compact dimension of 60 × 10 × 0.8 mm^3. A novel coverage strategy is proposed to utilize the loop mode for the low and the high bands (LTE700, GSM850, GSM900; LTE2300, WLAN, LTE2500) and the strip monopole mode for the medium band (DCS, PCS, UMTS). As a result, a nona-band coverage for 2G/3G/4G bands is achieved within limited space. Only one p–i–n diode is used with a simple bias circuit to avoid high insertion loss. With the proposed compact structure, the antenna is suitable for wideband smartphone applications. A prototype of the proposed antenna is fabricated and measured to verify the design strategy. The measured results match well with simulation with acceptable radiation efficiency in the covered bands. Especially, the efficiency in the low band is higher than 70%.**

***Index Terms*—Handset antennas, loop antennas, mobile antennas, monopole antennas, reconfigurable antennas.**

I. Introduction

With the rapid development of wireless technology, various 2G/3G/4G wireless communication standards with different operating frequencies have been proposed and deployed worldwide [1]. The handset antenna is demanded to cover multiple bands, including LTE700, GSM850, GSM900, DCS, PCS, UMTS, LTE2300, WLAN, and LTE2500 bands. In addition, the space for handset antennas especially for the nonground portion is much less due to the mainstream of large display and narrow frame in the smartphone [2]. Numerous kinds of antennas have been studied to fulfill the requirements of wideband and limited space, such as monopole antennas [2]–[4], slot antennas [5], [6], and loop antennas [7]–[9]. Moreover, a frequency reconfigurable antenna is another useful and effective method [10]–[15]. In this method, different operating modes are reconfigured in the same antenna structure without extra space. For instance, loop mode and planar inverted-F antenna (PIFA) mode in [10] and [11], loop mode and inverted-F antenna mode in [13], and loop mode and monopole mode in [14] are reconfigured, i.e., switched in a relatively small space or volume.

Manuscript received May 1, 2018; revised June 12, 2018 and July 10, 2018; accepted July 11, 2018. Date of publication July 16, 2018; date of current version August 2, 2018. This work was supported by the National Natural Science Foundation of China under Contract 61771280, and in part by the Beijing Natural Science Foundation under Contract 4182029. *(Corresponding author: Yue Li.)*

Y. Liu, P. Liu, and Y. Li are with the Department of Electronic Engineering, Tsinghua University, Beijing 100084, China (e-mail: liuyu2419@126.com; lpq14@mails.tsinghua.edu.cn; lyee@tsinghua.edu.cn).

Z. Meng and L. Wang are with the School of Aeronautic Science and Engineering, Beijing University of Aeronautics and Astronautics, Beijing 100191, China (e-mail: mengzhijun@buaa.edu.cn; wanglifeng@buaa.edu.cn).

Digital Object Identifier 10.1109/LAWP.2018.2856459

TABLE I
Performances of Mobile Handset Antennas

Reference	Area (mm^2)	Height of the non-ground portion (mm)	Covered Bands[a]
[3]	480	8	Octa-band
[4]	750	15	Nona-band
[5]	780	12	Nona-band
[6]	750	15	Nona-band
[7]	480	8	Octa-band
[8]	660	11	Octa-band
[9]	345	10	Nona-band
[12]	650	13	Nona-band
[15]	490	7	Nona-band
Proposed	**600**	**10**	**Nona-band**

[a]Octa-band: GSM850, GSM900, DCS, PCS, UMTS, LTE2300, WLAN and LTE 2500. Nona-band: LTE700, GSM850, GSM900, DCS, PCS, UMTS, LTE2300, WLAN and LTE 2500.

Especially, planar antenna modes such as PIFA mode and monopole mode are generally adopted for their compact, low-profile, and easily manufactured structure [12]. Nevertheless, PIFAs and monopole antennas exhibit the characteristic of a narrow bandwidth. In contrast, the loop mode is a favorable candidate in reconfigurable antennas for its multiresonant modes and wide bandwidth [16]. However, for the same operating frequency, the physical length of a loop resonator is larger than PIFAs and monopole antennas since the basic resonant mode in loop antennas is a half-wavelength mode but a quarter-wavelength mode in other antennas [11]. Therefore, it is challenging as well as important to embed the loop antenna in a limited planar space for multiple bands, especially for lower bands coverage.

In this letter, a planar printed reconfigurable antenna with the dimension of 60 × 10 × 0.8 mm^3 is proposed and studied. By using only one p–i–n diode, the proposed antenna combines the advantages of the loop antenna and the monopole antenna, namely, the loop mode and the strip monopole mode. Especially, we propose a new and feasible coverage strategy for reconfigurable antenna design, in which the loop mode successfully covers the low and the high bands (698–960 MHz, 2300–2690 MHz), and the strip monopole mode contributes to the medium band (1710–2170 MHz) coverage. Moreover, the proposed antenna achieves a quite high efficiency of over 70% in the low band. Additionally, the parasitic-element design is introduced in the strip monopole mode to broaden the bandwidth. Besides, a matching stub is also utilized to improve the bandwidth. To evaluate the performances of the proposed antennas, Table I compares the performances of some typical planar antennas and the proposed antenna. From Table I, we can obtain that the

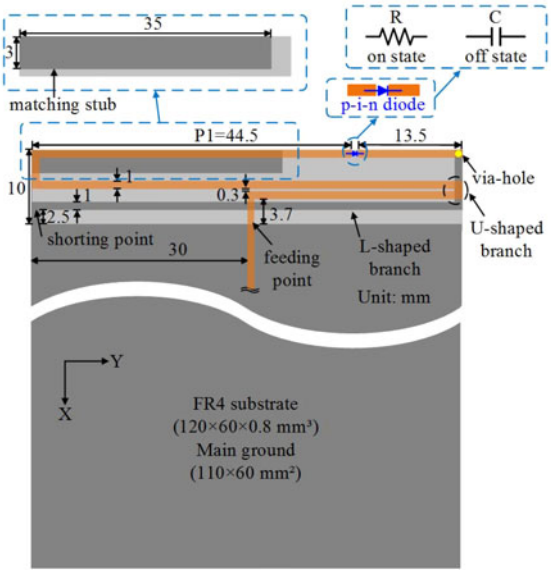

Fig. 1. General geometry and detailed dimensions of the proposed antenna.

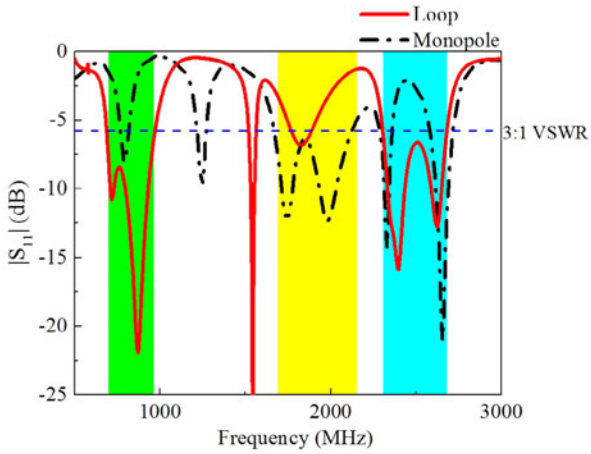

Fig. 2. Simulated $|S_{11}|$ of the loop and the monopole modes.

proposed antenna has an obvious advantage in the area, compared with antennas in [4]–[6]. Although the areas of antennas in [8] and [12] are close to the proposed antenna, their nonground portion heights, which are 11 or 13 mm, are larger than the height of the proposed antenna. The antennas in [3] and [7] have less area, but they do not cover the LTE700 band, which is the most difficult to be covered and crucial for LTE/WLAN mobile phones. It seems that the antenna in [9] achieves a better performance than the proposed antenna. However, the nona-band in [9] is utilized for tablet computers, which is mounted on a ground of $150 \times 200\,\text{mm}^2$. The antenna radiation performance can be significantly improved by the large-size ground, but it is not applicable for the limited space in handset antennas. As for the cubic antenna in [15], it takes a volume of $7 \times 70 \times 6\,\text{mm}^3$ to cover nine bands, which is not suitable for fabrication and slim design.

II. Antenna Configuration and Design

The geometry of the proposed nona-band reconfigurable antenna is shown in Fig. 1. A 0.8 mm thick FR4 substrate ($\varepsilon_r = 4.4$, $\tan\delta = 0.02$) is used as the system circuit board, and a main ground with a dimension of $110 \times 60\,\text{mm}^2$ is printed on the backside of the substrate. The loop antenna (uniform width of 1 mm) is folded and bent on both sides of 10 mm nonground portion, and the meander branch on the front connects the L-shaped branch on the backside through a via-hole. A 50 Ω microstrip line is arranged on the front side of the main board and is connected to the feeding point of the loop, while the main ground is connected to the shorting point of the loop with a short stub. For impedance matching, a matching stub with the width of 3 mm is printed at the corner of the system circuit board backside. A p–i–n diode is installed on the front branch, as illustrated in Fig. 1. Philips BAP64-03 silicon p–i–n diode is chosen for its good performance up to 3 GHz [17]. When the p–i–n diode is forward-biased, it works as a series resistance, and the antenna works in a typical loop mode for the low and high bands. Compared with the conventional switch, the p–i–n diode consumes large current and generates harmonics. However, for our proposed antenna, the insertion loss of the p–i–n diode is 0.1–0.2 dB at its typical forward current of 10–100 mA, which is acceptable for the system performance. On the other hand, the p–i–n diode works as a series capacitor with reverse-biased voltage; thus, the loop will be broken into two strips, and the antenna works in a strip monopole mode for the medium band. Fig. 1 also shows the equivalent circuit model of the p–i–n diode. The simulated $|S_{11}|$ performance for both working modes is illustrated in Fig. 2. A total of nine bands are covered with −6 dB (VSWR = 3:1) by combining two working modes. For the loop mode, LTE700, GSM850, GSM900, LTE2300, WLAN, and LTE2500 are covered. As for the strip monopole mode, DCS, PCS, and UMTS are covered. Since the p–i–n diode turns OFF at the strip monopole mode, we cut off the metal loop at the position of the p–i–n diode in the simulation. The commercial software Ansoft HFSS version 15.0 is used for simulation and parameter optimization.

III. Analyses of the Antenna

For the loop mode of the proposed antenna, a matching stub is utilized to improve the impedance matching of the high band, as shown in Fig. 1. To illustrate the impact of the matching stub, the high-band impedance curves of the loop mode with and without the matching stub are compared on the Smith chart in Fig. 3. As can be seen, with the matching stub, the impedance line of high-frequency bands is squeezed and generates a small circle in the −6 dB circle. According to the impedance matching in [18], the matching stub adds distributed shunt capacitance to the proposed antenna. Especially, the matching stub moves the impedance at 2695 MHz along the clockwise direction to hit the −6 dB circle. Moreover, it also moves the impedance over 2272 MHz into the matching area. Because of the series capacitance effects depending on the frequency, the matching stub broadens the high band greatly, with the additional coverage of LTE2300, WLAN, and LTE2500 bands.

To further understand working modes, the surface current distributions of the proposed antenna are shown in Fig. 4. Fig. 4(a) clearly shows that the current is the maximum at both feeding point and shorting point and the proposed antenna operates at a typical 0.5 λ loop mode at low frequency. As for the high frequency depicted in Fig. 4(c), four current nulls are observed. This indicates that the proposed antenna operates at a 2 λ loop mode. Furthermore, the matching stub introduces strong cou-

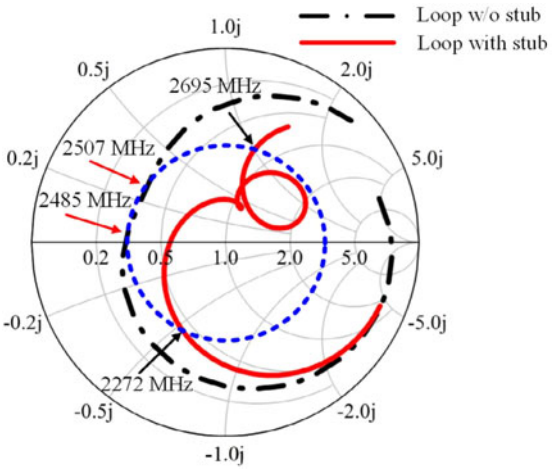

Fig. 3. Smith charts of the loop mode with and without the matching stub (for the high band: 2300–2690 MHz).

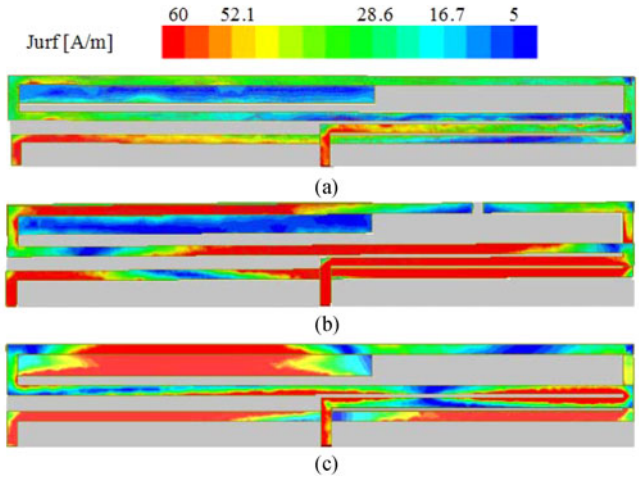

Fig. 4. Surface current distributions of the proposed antenna at (a) 740, (b) 1750, and (c) 2600 MHz.

pling at the higher frequency, proved by the dense current distribution on it at 2600 MHz. In the strip monopole mode, the 50 Ω microstrip line feeds the driven strip monopole, while the parasitic strip is fed by the direct power coupling from the driven strip monopole. Thus, the driven strip monopole is the main radiator, and the parasitic strip is utilized to widen the bandwidth. To be specific, Fig. 4(b) exhibits the current distribution at 1750 MHz for the strip monopole mode. According to the number of current nulls as well as the position of current extreme, the driven strip monopole operates at the 1.25 λ monopole mode, while the parasitic strip operates at the 0.75 λ monopole mode by coupling.

Based on the analysis mentioned above, it can be concluded that the low band can be covered by the typical 0.5 λ loop mode. Combining the 2 λ loop mode and coupling matching stub, the proposed antenna can cover the high band. Furthermore, in the strip monopole mode, both the driven strip monopole and the parasitic strip contribute their higher order resonant modes to achieve the medium band coverage.

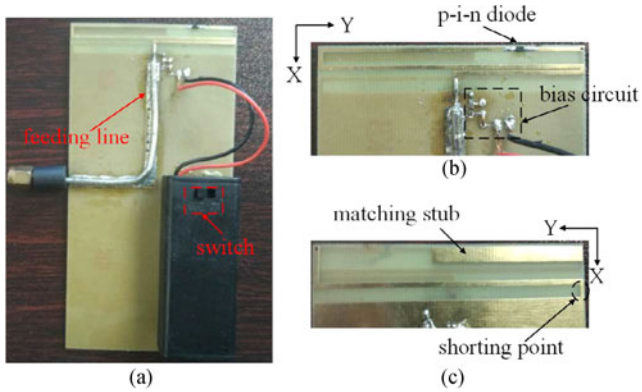

Fig. 5. Photograph of the fabricated antenna. (a) Front view. (b) Zoomed front view of the nonground portion. (c) Zoomed back view of the nonground portion.

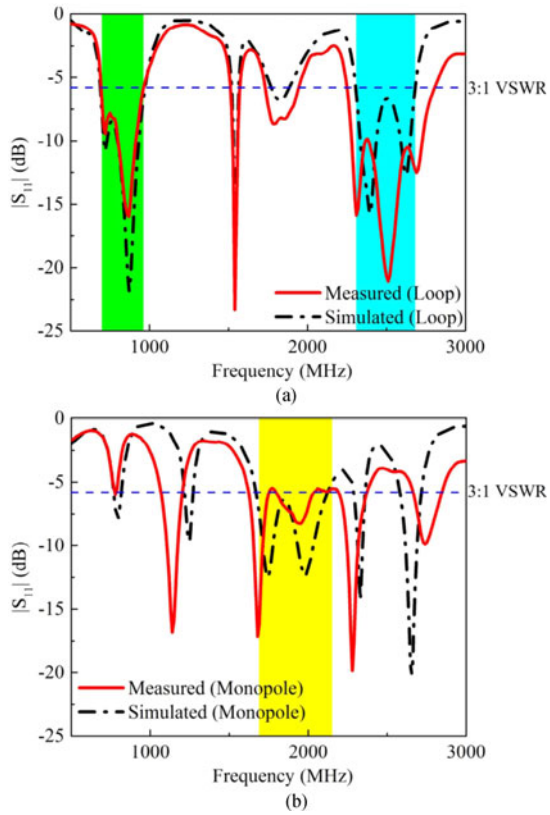

Fig. 6. Measured and simulated $|S_{11}|$ of (a) loop mode and (b) monopole mode.

IV. Antenna Fabrication and Measurement Results

To verify the analysis mentioned above, a prototype of the proposed antenna is fabricated and measured. Fig. 5 shows the front view of the fabricated antenna and the zoomed views of the nonground portion.

The comparison of measured and simulated $|S_{11}|$ of the proposed antenna is shown in Fig. 6. For results of the loop mode in Fig. 6(a), the measured result in the low band agrees well with the simulated result, and a bandwidth of 270 MHz (690–960 MHz) is achieved. Moreover, thanks to the 1 λ loop mode, a part of the L-band in LTE is also covered from

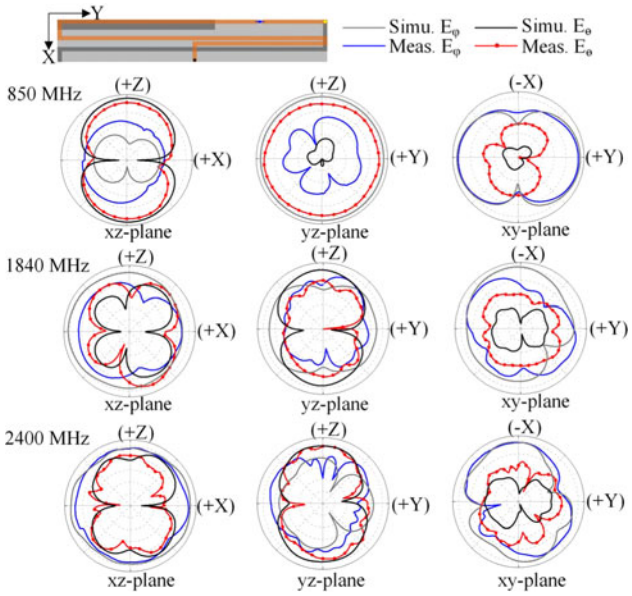

Fig. 7. Measured and simulated radiation patterns of the proposed antenna.

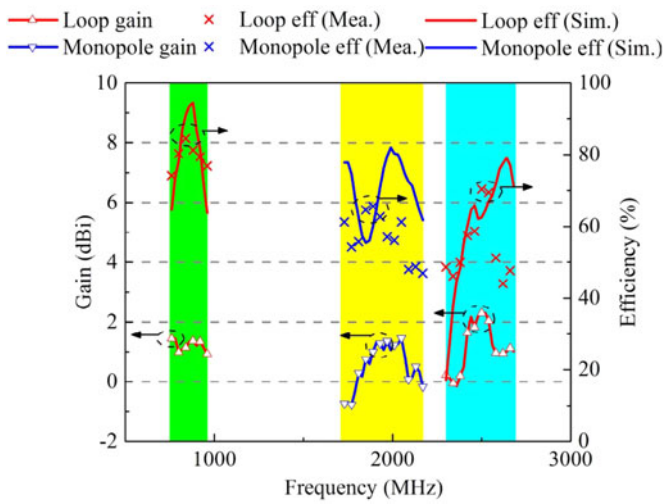

Fig. 8. Measured and simulated efficiency and measured gain.

1510 to 1580 MHz. Besides, three high-order resonant modes are observed in measured results of the high band, which is different from two resonant modes in simulated results. This is mainly because of the sensitivity of the matching stub to the physical losses. Fortunately, the increased resonant mode broadens the bandwidth. As a result, a wide bandwidth of 540 MHz (2260–2800 MHz) is achieved. Therefore, the measured $|S_{11}|$ of the loop mode covers LTE700/GSM850/GSM900/LTE2300/WLAN/LTE2500 bands. As for the results of the strip monopole mode in Fig. 6(b), in the medium band, the operating frequencies have small shifting compared with the simulated results. The difference between the measured and simulated results is mainly caused by fabrication error and measurement error. Despite this, the strip monopole mode achieves a bandwidth of 410 MHz (1620–2030 MHz), covering DCS/PCS/UMTS bands.

Fig. 7 exhibits the measured and simulated normalized radiation patterns in three principal planes. To evaluate the effect in different bands, three typical frequencies are selected and plotted. The measured results generally agree with the simulated results. At 850 MHz, the radiation patterns show dipole-like patterns according to the omnidirectional radiation in the *yz* plane. As for the medium and the high bands, the radiation patterns become complicated with more variations and nulls observed. The reason for the phenomenon is because of the proposed antenna operating in a high-order mode in the medium- and high-frequency bands.

The radiation efficiency gain of the proposed antenna is shown in Fig. 8. Since the measured anechoic chamber does not satisfy the far-field condition in part of the low band, we omit the inaccurate results below 750 MHz. The measured results agree well with the simulated results, which proves the accuracy of the measurement. Besides, it can be observed that the measured radiation efficiency varies from 70% to 84% in the low band. For the medium and the high bands, the radiation efficiency is better than 40%. Moreover, high-quality diodes used in the practical applications can improve the radiation efficiency significantly. It is worth mentioning that the current cancellation makes the radiation efficiency in the medium- and high-frequency bands lower than the efficiency in the low-frequency band. Meanwhile, the measured gain ranges from 0.50 to 1.45 dBi in the low band, and the measured gain is better than 0.20 dBi in most of the medium and high bands. The measured efficiency and gain are acceptable in the practical applications.

V. Conclusion

In this letter, a planar nona-band reconfigurable antenna with the dimension of $60 \times 10 \times 0.8\,\text{mm}^3$ is proposed. By using only one p–i–n diode for a mode switch, we design a novel coverage strategy, in which the loop mode is utilized for the low and the high band coverage, while the strip monopole mode achieves the medium band coverage. A matching stub is added in the loop mode, and the parasitic design is adopted in the monopole mode. These two methods greatly improve the bandwidth performance. The prototype antenna is fabricated and measured. As a result, the proposed antenna covers LTE700, GSM850, GSM900, DCS, PCS, UMTS, LTE2300, WLAN, and LTE 2500 bands with good radiation performance.

References

[1] Z. Ying, "Antennas in cellular phones for mobile communications," *Proc. IEEE*, vol. 100, no. 7, pp. 2286–2296, Jul. 2012.

[2] R. Tang and Z. Du, "Wideband monopole without lumped elements for octa-band narrow-frame LTE smartphone," *IEEE Antennas Wireless Propag. Lett.*, vol. 16, pp. 720–723, 2017.

[3] C. J. Deng, Y. Li, Z. J. Zhang, and Z. H. Feng, "A novel low-profile hepta-band handset antenna using modes controlling method," *IEEE Trans. Antennas Propag.*, vol. 63, no. 2, pp. 799–804, Feb. 2015.

[4] J. Ilvonen, R. Valkonen, J. Holopainen, and V. Viikari, "Design strategy for 4G handset antennas and a multiband hybrid antenna," *IEEE Trans. Antennas Propag.*, vol. 62, no. 4, pp. 1918–1927, Apr. 2014.

[5] C. K. Hsu and S. J. Chung, "Compact antenna with U-shaped open-end slot structure for multi-band handset applications," *IEEE Trans. Antennas Propag.*, vol. 62, no. 2, pp. 929–932, Feb. 2014.

[6] Z. Chen, Y. L. Ban, J. H. Chen, J. L. W. Li, and Y. J. Wu, "Bandwidth enhancement of LTE/WWAN printed mobile phone antenna using slotted ground structure," *Prog. Electromagn. Res. Lett.*, vol. 129, no. 7, pp. 469–483, Jul. 2012.

[7] P. Wang and Z. Q. Cai, "Planar printed loop antenna with less no-ground space for hepta-band wireless wide area network/long-term evolution mobile handset," *Electron. Lett.*, vol. 52, no. 15, pp. 1284–1286, Jul. 2016.

[8] W. S. Chen *et al.*, "A compact loop antenna for 4G mobile system," in *Proc. IEEE Antennas Propag. Soc. Int. Symp.*, 2013, pp. 1712–1713.

[9] K. L. Wong and M. T. Chen, "Small-size LTE/WWAN printed loop antenna with an inductively coupled branch strip for bandwidth enhancement in the tablet computer," *IEEE Trans. Antennas Propag.*, vol. 61, no. 12, pp. 6144–6151, Dec. 2013.

[10] Y. Li, Z. J. Zhang, J. F. Zheng, and Z. H. Feng, "Compact heptaband reconfigurable loop antenna for mobile handset," *IEEE Antennas Wireless Propag. Lett.*, vol. 10, pp. 1162–1165, 2011.

[11] Y. Sung, "Multi-band reconfigurable antenna for mobile handset applications," *Microw., Antennas Propag.*, vol. 8, no. 11, pp. 864–871, Mar. 2014.

[12] S. W. Lee, H. S. Jung, and Y. J. Sung, "A reconfigurable antenna for LTE/WWAN mobile handset applications," *IEEE Antennas Wireless Propag. Lett.*, vol. 14, pp. 48–51, 2015.

[13] Y. Li, Z. J. Zhang, J. F. Zheng, Z. H. Feng, and M. F. Iskander, "A compact hepta-band loop-inverted F reconfigurable antenna for mobile phone," *IEEE Trans. Antennas Propag.*, vol. 60, no. 1, pp. 389–392, Jan. 2012.

[14] M. G. S. Hossain and T. Yamagajo, "Reconfigurable printed antenna for a wideband tuning," in *Proc. 4th Eur. Conf. Antennas Propag.*, Barcelona, Spain, Apr. 2010, pp. 1–4.

[15] C. H. Chang, C. M. Lee, and H. Y. Wang, "Simple tunable Inverted-F antenna for LTE/WWAN mobile handset applications," in *Proc. 5th Asia-Pacific Conf. Antennas Propag.*, Kaohsiung, Taiwan, Jul. 2016, pp. 401–402.

[16] M. Zheng, H. Y. Wang, and Y. Hao, "Internal hexa-band folded monopole/dipole/loop antenna with four resonances for mobile devices," *IEEE Trans. Antennas Propag.*, vol. 60, no. 6, pp. 2880–2885, Jun. 2012.

[17] NXP Semiconductors, "Datasheet of BAP64-03 silicon PIN diode," 2015. [Online]. Available: http://www.hytic.net/upload/files/2018/06/NXP-BAP64-03.pdf

[18] Z. J. Zhang, "Antenna matching," in *Antenna Design for Mobile Devices*. Hoboken, NJ, USA: Wiley, 2011, pp. 19–58.